

CONTROL OF LASER RADIATION PARAMETERS

PACS numbers: 42.55.Px; 42.62.Eh; 42.79.Jq; 42.25.Fx
DOI: 10.1070/QE2012v042n04ABEH014646

Laser frequency stabilisation by the Pound–Drever–Hall method using an acousto-optic phase modulator operating in the pure Raman–Nath diffraction regime

V.N. Baryshev

Abstract. **Frequency stabilisation of diode laser radiation has been implemented by the Pound–Drever–Hall method using a new acousto-optic phase modulator, operating in the pure Raman–Nath diffraction regime. It is experimentally shown that, as in the case of saturated-absorption spectroscopy in atomic vapour, the spatial divergence of the frequency-modulated output spectrum of this modulator does not interfere with obtaining error signals by means of heterodyne frequency-modulation spectroscopy with a frequency discriminator based on a high-Q Fabry–Perot cavity with finesse of several tens of thousands.**

Keywords: *diode laser, optical heterodyne frequency-modulation spectroscopy, Pound–Drever–Hall laser frequency stabilisation, acousto-optic modulator, Raman–Nath diffraction, Fabry–Perot cavity.*

1. Introduction

The Pound–Drever–Hall (PDH) method is, without exaggeration, the most powerful tool for frequency stabilisation of modern lasers [1]. It has been developed based on optical heterodyne frequency-modulation (FM) spectroscopy [2, 3] (used for phase-sensitive detection of optical resonances) and utilises a high-efficiency optical frequency discriminator (Fabry–Perot interferometer) and a laser stabilisation scheme based on it.

The PDH method is simple and efficient. It implies heterodyne detection of resonant radiation reflected from a Fabry–Perot cavity (FPC) and formation of an error signal for feedback loops (which is a derivative of radiation intensity with respect to frequency). In the case of diode lasers, the bandwidth of the injection current feedback loop can exceed 10 MHz. This circumstance allows one to reduce the spectral width of diode laser radiation (when locked to a high-Q FPC) to sub-Hertz values [4]. Note that the possibility of the diode laser spectrum narrowing to the level of a few Hertz by means of phase locking to the high-Q cavity resonance was considered in [5] not long before the implementation of heterodyne frequency-modulation PDH technique or simultaneously with it.

V.N. Baryshev Federal State Unitary Enterprise 'National Research Institute for Physicotechnical and Radio Engineering Measurements', 141570 Mendeleevo, Moscow region, Russia;
e-mail: baryshev@vniiftri.ru

Received 13 September 2011; revision received 6 March 2012
Kvantovaya Elektronika **42** (4) 315–318 (2012)
Translated by Yu.P. Sin'kov

This study is devoted to the frequency stabilisation of diode lasers. To this end, we used the PDH method with a new acousto-optic modulator, operating in the pure Raman–Nath diffraction regime (AOM-RN). The only seeming disadvantage of AOM-RN is the spatial divergence of its frequency-modulated output spectrum. We have shown experimentally that, as in the case of saturated-absorption spectroscopy [6, 7], this divergence is not an obstacle for obtaining the error signals by means of the PDH method with a frequency discriminator based on a high-Q Fabry–Perot cavity with finesse of several tens of thousands.

2. Experimental setup and the results of experiment

A schematic of the experimental setup for obtaining error signals by the PDH method is presented in Fig. 1. It was shown in [6] that AOM-RN can be used as an external phase modulator in the PDH method to transform single-frequency radiation of an external-cavity diode laser (ECDL) into a frequency-modulated spectrum. A new AOM-RN sample, operating in the pure Raman-Nath diffraction regime, was presented in [7]. As follows from [6, 7], its application as an external phase modulator has a number of advantages over the case where an electro-optical modulator (EOM) is used for phase modulation. Error signals with a desired slope of their linear central part in a wide frequency range are obtained by simple variation in the frequency of amplified signal from a local RF oscillator, which is applied to AOM-RN without changing the signal power. This power, sufficient to provide an intensity ratio of several percent for the diffracted beams of the ±1st and zero orders, did not exceed 100 mW. Since the existing EOMs do not produce a pure FM spectrum, one has to control the polarisation of the input and output beams in order to remove the residual amplitude noise. When using AOM-RN, such control is not required and the experimental setup is simplified. The spatial divergence of the AOM-RN output radiation (i.e., the beams corresponding to the carrier and to the nearest ±1st diffraction order sidebands) was not a severe obstacle or inconvenience for obtaining the error signals corresponding to saturated-absorption resonances in caesium vapour [7]. We will show below that the divergence of output AOM-RN radiation is not an obstacle in the more complex experiment: formation of error signals corresponding to the resonances of high-Q Fabry–Perot cavities, which are used as frequency discriminators in PDH frequency-modulation spectroscopy.

The AOM-RN developed at the National Research Institute for Physicotechnical and Radio Engineering

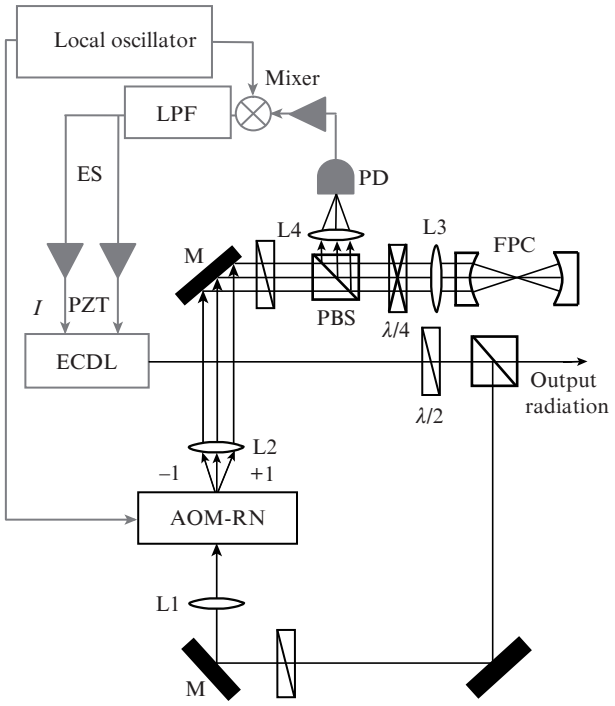

Figure 1. Schematic of the experimental setup: (ECDL) external-cavity diode laser, (PBS) polarising beam splitter, ($\lambda/2$) half-wave plate, ($\lambda/4$) quarter-wave plate, (L) lens, (M) mirror, (PD) photodetector, (LPF) low-pass filter, (PZT) piezo-electric transducer, (I) laser diode injection current, (FPC) Fabry–Perot cavity, and (ES) error signal.

Measurements (VNIIFTRI) had an acousto-optic interaction length of 2 mm, central modulation frequency of about 30 MHz, and a modulation bandwidth of 20 MHz; it provided an FM spectrum of single-mode ECDL radiation at a wavelength of 689 nm. Note that radiation at this wavelength is used in the optical frequency standards based on strontium atoms (^{87}Sr, ^{88}Sr) in an optical lattice (in the second stage of cooling of the atoms on the narrow $^1S_0 - {}^3P_1$ transition) [8, 9]. The natural width of this transition is 7.5 kHz; therefore, the instantaneous spectral width of ECDL radiation must be of the same order of magnitude; this circumstance requires frequency locking to the high-Q optical cavity by means of the PDH method. Long-term stability of ECDL can be provided by FM saturated-absorption spectroscopy in strontium vapour, using again AOM-RN as a phase modulator [7].

Thus, the output AOM-RN spectrum (Fig. 1) consists of a carrier signal at a frequency ω_{ECDL} and two sidebands, corresponding to the ±1st diffraction order, with frequencies $\omega_{ECDL} \pm \Omega$, where Ω is the AOM-RN modulation frequency [7]. It is not necessary to align exactly the AOM-RN position due to the following specific feature of Raman–Nath diffraction: if the acousto-optic interaction length is sufficiently small, this diffraction occurs at any angle of incidence of light on an acoustic beam (in contrast to the Bragg diffraction, which occurs only at a certain angle of incidence of optical wave, satisfying the Bragg condition). When an AOM-RN is placed in a telescopic system formed by lenses L1 and L2 (Fig. 1), the radiation arriving at a confocal FPC consists of three collimated parallel beams. A matching lens L3 focuses the input radiation approximately to the point in the middle between the FPC mirrors. A commercial confocal FPC SA200-5B (Thorlabs) with finesse $F \approx 200$ and $\Delta_{FSR} = 1.5$ GHz was used as a frequency discriminator. The identical spherical mirrors forming this cavity are spaced by a distance equal to the radius of curvature of the mirrors. The power of the beam that arrives at the FPC and has a size of 2 mm in the horizontal plane (in which all three parallel light beams lie) is 1.25 mW. The radiation reflected from the FPC with the aid of a quarter-wave plate, a polarising beam splitter, and a collecting lens L4 is deviated and focused onto a fast photodetector.

The radiation arriving at the photodetector is the sum of several light beams: three beams corresponding to the FM spectrum of AOM-RN output radiation (which did not enter the cavity but were reflected from the input FPC mirror) and the beam reflected from the FPC, which is a part of the standing light wave formed in the FPC when the frequency of any spectral component matches the resonant frequency of the cavity. The FPC transmission bandwidth Δ_{FSR}/F was 7.5 MHz, and the total power arriving at the photodetector was 0.88 mW. An optical wave at the laser carrier frequency ω_{ECDL}, when matched with the FPC resonant frequency, forms an intracavity standing wave at this frequency. Since the FPC input mirror is not a perfect reflector, the standing wave penetrates partially this mirror toward the radiation that is incident on the cavity. The wave emerging from the cavity in the backward direction and the wave reflected from the input mirror have equal amplitudes at the carrier frequency and are in antiphase, which leads to their mutual compensation at the exact resonance and to the zero beat signal (on the photodetector) at the AOM-RN modulation frequency Ω. The heterodyne (with respect to the signal of the local oscillator) detection of the beat signal yields an error signal, which contains information about the laser radiation frequency and phase and has a form corresponding to the in-phase component (sin Ωt component) of the beat signal [2, 3, 7].

Figure 2 shows the error signal and the FPC transmission signal, recorded simultaneously when scanning the laser frequency ω_{ECDL}; the scanning was performed by applying a saw-tooth voltage to a piezo-electric transducer, which controlled the length of the ECDL external cavity. The AOM-RN

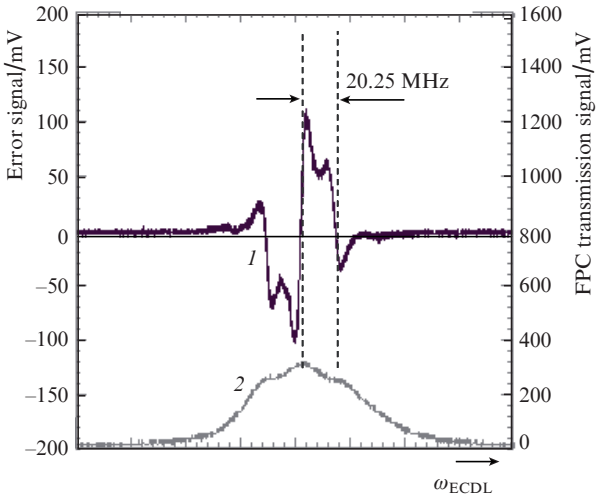

Figure 2. (*1*) Error signal and (*2*) transmission signal of confocal FPC, recorded simultaneously when scanning the ECDL frequency ω_{ECDL}. The AOM-RN modulation frequency Ω is 20.25 MHz.

modulation frequency Ω was 20.25 MHz. The transmission signal was recorded by a photodiode located behind the FPC output mirror. Curve (*2*) includes three transmission signals, which correspond to the three resonances, formed successively at the frequencies of first sideband, carrier, and second sideband. The widths of these three signals depend not only on the FPC resolution but also on the modulation frequency Ω and the ECDL frequency scanning rate. When recording the data in Fig. 3, the modulation frequency was increased to 47.09 MHz, while the scanning parameters remained the same. When the modulation frequency is varied continuously from 20 to 50 MHz the sign of the error signal slope changed several times (successively and periodically). This modulation frequency range also makes it possible to obtain multiply an error signal with zero background, as shown in Figs 2 and 3.

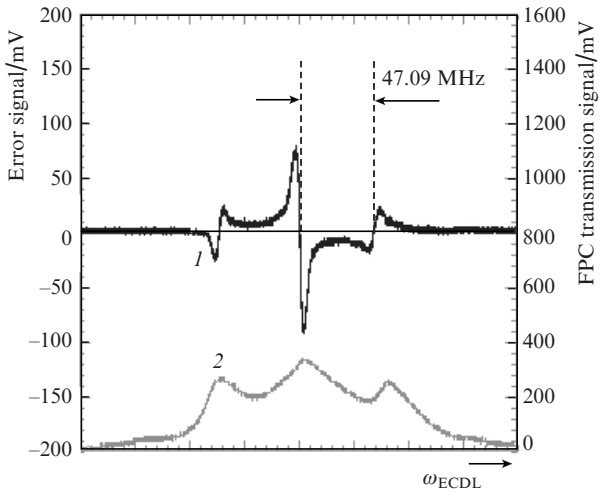

Figure 3. (*1*) Error signal and (*2*) transmission signal of confocal FPC, recorded simultaneously when scanning the ECDL frequency ω_{ECDL}. The AOM-RN modulation frequency Ω is 47.09 MHz.

Since the beat signal on the photodetector is proportional to the geometric mean value of the carrier power P_c and the power P_s of some sideband, one can maximise the error signal and increase the slope of its central part by changing the power of the signal from the local oscillator, which is applied to AOM-RN. With all other diffraction orders (except for the first one) neglected, i.e., at the total ECDL radiation power $P_0 = P_c + 2P_s$, the value $(P_cP_s)^{1/2}$ will be maximum at $P_s/P_c = 1/2$ and $P_s = 1/4P_0$. This ratio of the power diffracted into the first order by AOM-RN and the carrier power exceeds several times their ratio (few percent) that was found to be sufficient to implement saturated-absorption spectroscopy in caesium vapour [6, 7]. This ratio is not critical for AOM-RN functioning.

In the same experimental configuration (Fig. 1), an ultrastable and super-high-Q FPC with finesse $F \approx 60000$ and $\Delta_{FSR} = 1.92$ GHz was used as a frequency discriminator. The optical elements of this cavity were made of a material with an ultralow coefficient of thermal expansion (ULE cavity). The design of this cavity, which is a part of the optical system for the optical frequency standard on strontium atoms in optical lattice that is being developed at VNIIFTRI, as well as this standard, will be described elsewhere. The error signal with zero background [Fig. 4, curve (*1*)] was used to stabilise the ECDL frequency by the resonance of this super-high-Q FPC. A part of radiation at the AOM-RN output (composed, as previously, of the carrier and two sidebands of the first diffraction order) was introduced into a single-mode polarisation-maintaining fibre and directed to the ULE cavity (Fig. 5). The AOM-RN modulation frequency was 19.99 MHz, and the total power of the light beams at the fibre output was 0.34 mW. When scanning the ECDL frequency ω_{ECDL}, curve (*1*) exhibits three regions where the dispersion-like shaped error signals were formed at successive coincidence of the upper sideband, carrier, and lower sideband frequencies with the ULE cavity resonant frequency [Fig. 4, curve (*2*)].

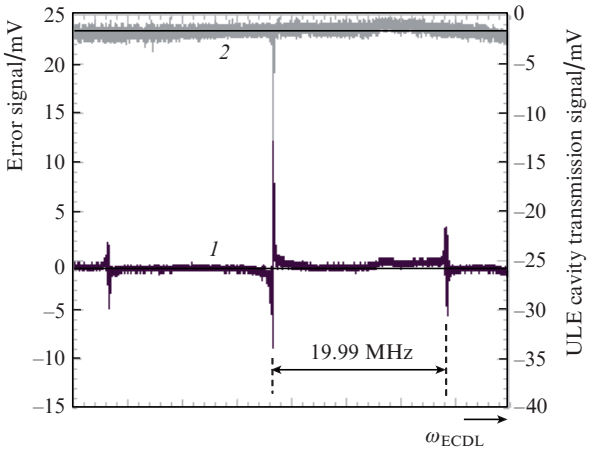

Figure 4. (*1*) Error signal and (*2*) transmission signal of high-Q ULE cavity, recorded simultaneously when scanning the ECDL frequency ω_{ECDL}. The AOM-RN modulation frequency Ω is 19.99 MHz.

Figure 6 shows a beat signal at 520 MHz between two ECDLs, locked separately to the resonances of SA200-5B Fabry–Perot cavity and ULE cavity. The full width at half maximum $\Delta\nu$ of this beat signal, which does not exceed 100 kHz, is determined mainly by the spectral width of the ECDL radiation locked to FPC SA200-5B resonance. Both these devices were placed on an optical table that was not mechani-

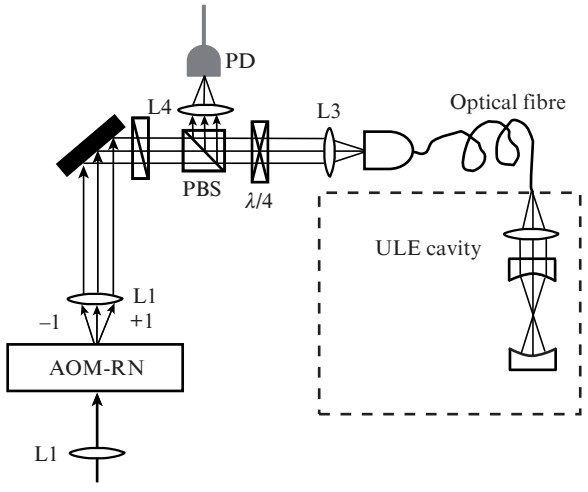

Figure 5. Part of the experimental setup with an optical fibre and ULE cavity (finesse of 60000).

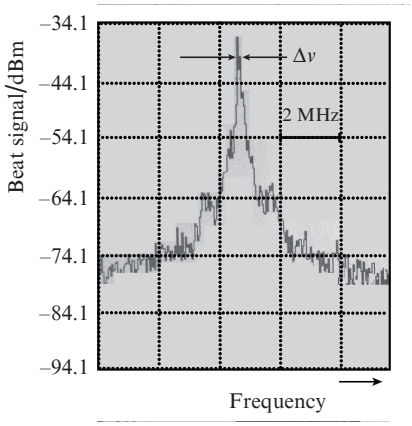

Figure 6. Beat signal of the radiation of two ECDLs, locked separately to resonances of the SA200-5B Fabry–Perot cavity and the ULE cavity.

cally and acoustically isolated. The ECDL radiation spectrum width in the free-running regime exceeds 1 MHz.

3. Conclusions

This paper completes the series of studies devoted to the experimental demonstration and justification for applying AOM-RN as a phase modulator in frequency-modulation heterodyne spectroscopy of optical resonances, such as saturated-absorption resonances and narrow resonances of coherent population trapping. We used the PDH method with a new acousto-optic modulator, operating in the pure Raman–Nath diffraction regime, as an optical phase modulator for frequency stabilisation of the diode lasers. It is experimentally shown that the divergence of AOM-RN output radiation, i.e., the beams corresponding to the carrier and nearest sidebands of the ±1st diffraction order, is not an obstacle in more complex experiments, where the error signals corresponding to the resonances of high-Q Fabry–Perot cavities are obtained. The AOM-RN, which was developed to be used as an external phase modulator in frequency-modulation spectroscopy, has the following advantages over electro-optical modulators: compactness, low energy consumption, wide range of modulation frequencies, and the absence of necessity to control the input and output polarisations. This design has never been used previously for the aforementioned purpose. The development of AOM-RN extended the set of tools that are used as external phase modulators in laser spectroscopy.

References

1. Drever R.W., Hall J.L., Kovalski F.V., Hough J., Ford G.M., Munley A.J., Ward H. *Appl. Phys. B*, **31**, 97 (1983).
2. Bjorklund G., Levenson M., Lenth W., Ortiz C. *Appl. Phys. B*, **32**, 145 (1983).
3. Bjorklund G.C. *Opt. Lett.*, **5**, 15 (1980).
4. Notcutt M., Ma L.-S., Ye J., Hall J.L. *Opt. Lett.*, **30**, 1815 (2005).
5. Belenov E.M., Velichanskii V.L., Zibrov A.S, Nikitin N.N., Sautenkov V.A., Uskov A.V. *Kvantovaya Elektron.*, **10** (6), 1232 (1983) [*Sov. J. Quantum Electron.*, **13** (6), 792 (1983)].
6. Baryshev V.N., Domnin Yu.S., Kopylov L.N. *Kvantovaya Elektron.*, **37** (11), 1006 (2007) [*Quantum Electron.*, **37** (11), 1006 (2007)].
7. Baryshev V.N., Epikhin V.M. *Kvantovaya Elektron.*, **40** (5), 431 (2010) [*Quantum Electron.*, **40** (5), 431 (2010)].
8. Katori H., Ido T., Isoya Y., Kuwata-Gonokami M. *Phys. Rev. Lett.*, **82**, 1116 (1999);
9. Mukaiyama T., Katori H., Ido T., Li Y., Kuwata-Gonokami M. *Phys. Rev. Lett.*, **90**, 113002 (2003).